Development of Aircraft Diesel Engine
for Military Use

P. Novotný[*], V. Píštěk, L. Drápal and R. Ambróz

[1]Brno University of Technology, Institute of Automotive Engineering

Abstract:

The paper deals with the cranktrain development of a new diesel engine for possible military use. The engine utilized potentials are discussed at the beginning of the paper. The cranktrain vibration and fatigue are solved by computational approaches. The computational model incorporating flexible bodies is assembled and solved in Multi-Body System. Slide bearings are solved by a hydrodynamic approach. The results include vibrations of the cranktrain and also fatigue analyses of cranktrain key parts, such as crankshafts or a propeller shaft. There are also presented design modifications enabling reduction of vibrations and fatigue increase of main parts.

1. Introduction

After all efforts in the area of alternative powertrains, the piston internal combustion engines are expected to be globally dominant in the next years. The modern engines are subjected to strict performance parameters, weight restrictions, fuel consumption restrictions and reliability requirements. Historically the efforts to combine these requirements introduced two-stroke diesel supercharged engines. The most famous engine of this category during the thirties and at the beginning of the forties of the twentieth century was Junkers Jumo 204-208 developed by this famous German producer [4].

The potential low power specific weight and high box size specific power of the two-stroke diesel supercharged engines make it attractive for niche markets, such as:

- Military/commercial aircraft or helicopters
- Military generator sets

---

[*] *Corresponding author: Institute of Automotive Engineering, Faculty of Mechanical Engineering, Brno University of Technology, Technická 2, 616 69, Brno, Czech Republic, +420 541 142 272, novotny.pa@fme.vutbr.cz*

- Utility & Constructions generator sets
- Mobile trailer mounted generator sets
- APU – Auxiliary Power Units
- UAV – Unmanned Aircraft

1.1. Aircraft Engine Requirements

Aircraft are one of the most challenging applications for engines, presenting a lot of design requirements, many of which conflict with each other. In general, the aircraft engine must be:

- Reliable, as losing power in an airplane is a substantially greater problem than in an automobile. The aircraft engines operate at temperature, pressure and speed extremes, and therefore need to achieve reliability and safeness under different conditions.
- Lightweight, as the engine weight increases, the empty weight of the aircraft decreases and the aircraft payload is reduced.
- Powerful to overcome the weight and drag of the aircraft.
- Small and easily streamlined because large engines with large surface area create too much drag.
- Field repairable to keep the cost of replacement down. Minor repairs should be relatively inexpensive.
- Fuel efficient to give the flying range according to the aircraft design requirements.
- Capable of operating at sufficient altitude for the aircraft.

Unlike automobile engines, aircraft engines are often operated at high power settings for extended periods of time. In general, the engine runs at maximum power for a few minutes during taking off and then engine power is reduced for a climb, and then spends the majority of its time at a cruise setting, typically from 65 % to 75 % of full power. In contrast, an automobile engine might spend 20 % of its time at 65% power while accelerating, followed by 80 % of its time at 20% power while cruising.

The design of aircraft engines tends to favour reliability over performance. Long engine operation times and high power settings, combined with the requirement for high reliability need precise construction. Aircraft engines tend to use the simplest parts possible and include two sets of anything needed for reliability. Independence of function lessens the likelihood of a single malfunction causing an entire engine to fail. For example, reciprocating engines have two independent magneto ignition systems, and the engine mechanical engine-driven fuel pump is always backed-up by an electric pump.

Aircraft operate at higher altitudes where the air is less dense than at ground level. As engines need oxygen to burn fuel, a forced induction system such as a turbocharger or supercharger is especially appropriate for aircraft use. This brings, along the usual drawbacks of additional cost, weight and complexity.

1.2. Military Generator Set Requirements

The military generator sets have a unique set of requirements which significantly differ from commercial generator sets. The primary requirements can be characterised as:

- Robustness, transportability, reliability, maintainability.
- All-range diesel fuel capability.

- 50, 60, 400 Hz mode flexibility (utility and precise electrical power quality), as well as 120/240V capability.
- Operation in severe environmental conditions. Full altitude rating at 1500 m and 35 °C, with a power factor of 0.8. Operation at extreme temperature range from -45 °C to +50 °C (storability from -50 °C to +70 °C). Ability to withstand extreme solar loading, wind, rain, ice, dust, sand and humid conditions.

Other unique military requirements include:

- Transportability - rail, road and aircraft (including helicopter).
- EMI - electromagnetic interference characteristics (also for low battlefield susceptibility).
- EMP - protection against high amplitude electromagnetic pulse bursts.
- NBC - capability of withstanding nuclear, biological and chemical agents, and subsequent decontamination procedures.
- Ability to be operated by soldiers in heavy, bulky arctic and NBC protective clothing.

2. Target Engine

2.1. General Description

The target engine originates from a supercharged diesel engine with two opposite crankshafts. The engine is presented in Figure 1.

Fig. 1 Target engine

Both of the crankshafts include two crank pins rotated reciprocally by 180°. Two connecting rods and two pistons are therefore connected to every crankshaft. The pistons of opposite crank pins move against each other in a common liner, the arrangement is two-cylinder engine. The crankshafts are coupled by a spur gear drive. The spur gear drive is simultaneously used as a reducer enabling a propeller speed decrease. This arrangement is utilized because of engine compactness accompanying resulted light weight. Two-stroke supercharged diesel engines introduce the best values of specific effective fuel consumption. This is conditioned by a suitable design of the timing subsystem. The target engine includes uniflow scavenging enabling to fine scavenge a combustion chamber. Inlet and exhaust ports are covered up by pistons of the first and second crankshaft, thence the crankshafts are called the intake and the

exhaust crankshaft. It has to be noticed that due to uniflow scavenging principles the timing diagram is non-symmetrical and the rotation of the intake crankshaft is delayed by a defined angle in comparison with the exhaust crankshaft. The engine power output is also increased by the application of a turbocharger combined by a supercharger. The supercharger is required mainly for an engine start-up [4].

2.2. Cranktrain Balancing Analysis

Preliminary balancing analysis used in this relatively uncommon concept shows that the size of the resultant of inertia forces in rotating mass is zero, however, their momentum vector is non-zero, has a constant size in static regime and is rotating as crankshafts. Such effect can be reduced by using a balance weight placed on the crankshafts, or should be taken into consideration when designing the bedding of the engine in the frame [4].
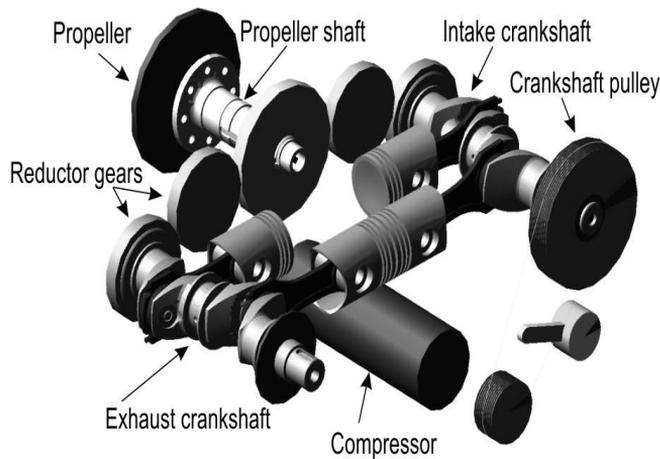

Fig. 2 Target engine cranktrain description

The resultant of the first-order inertia forces of reciprocating masses is zero while their moment vector is non-zero, takes a sinusoidal pattern and tends to turn by the whole aggregate around the axis perpendicular to the cylinder plane. Balancing can be done by two balancing shafts running in opposed direction or it can be adjusted in the engine bedding.

The resultant of the second-order inertia forces of reciprocating masses and their moments are non-zero, they oscillate sinusoidally with double frequency compared with the frequency of crankshaft rotation, and the forces result in vibrations of the whole aggregate in direction of the cylinder axes and the momentums then turn it in the same way as in the first-order case, but with a double frequency.

Non-zero resultants of the given flywheel effects of the whole aggregate are caused by mutual angular crankshaft mismatch which is necessary for proper function of scavenging. But the higher the angular mismatch, the worse the engine balancing is. Such flywheel effects can be partially or totally eliminated by the use of balancing shafts (except for the momentums of flywheel forces in rotating mass), which however increases the total engine weight and complexity. That is why a thorough adjustment of the engine bedding in the frame seems more suitable [4].

3. Cranktrain Dynamic Solution Approach

The existing conception of the target engine including knowledge of main dimensions enables to use modern computational methods for a cranktrain dynamic and fatigue solution, known as virtual engine. The virtual engine is a complex computational model based on MBS (Multi-Body System) principles in combination with FEM (Finite Element Method).

3.1. Theory Background of Flexible Bodies

Flexible bodies represented by FE (Finite Element) models have decisive importance for powertrain dynamics simulations. The FE models of each component should be created with special effort and the uniform FE mesh is often preferred. ANSYS is used for all FE calculations.

In general, for solution in time domain, FE models are very large and require reduction. The discretization of a flexible component into a finite element model represents the infinite number of DOF (Degrees of freedom) with a finite, but very large number of finite DOF. The linear deformations of the nodes of this FE model, u, can be approximated as a linear combination of a smaller number of shape vectors

$$u = \sum_{i=1}^{M} \Phi_i q_i \quad , \tag{1}$$

where M is number of mode shapes, Φ_i is mode shape and q_i are modal coordinates [1].

For reduction of FE models, the Craig-Bampton method is used. The Craig-Bampton method separates the system DOF into boundary DOF, u_B, and interior DOF, u_I. Two sets of mode shapes are defined as follows:

- Constrain modes: these modes are static shapes obtained by giving each boundary DOF a unit displacement while holding all other boundary DOFs fixed.
- Fixed-boundary normal modes: these modes are obtained by fixing the boundary DOF and computing an eigenvalue solution.

The relationship between the physical DOF and Craig-Bampton modes and their modal co-ordinates is illustrated by the following equation

$$u = \begin{pmatrix} u_B \\ u_I \end{pmatrix} = \begin{pmatrix} I & 0 \\ \Phi_{IC} & \Phi_{IN} \end{pmatrix} \begin{pmatrix} q_C \\ q_N \end{pmatrix}. \tag{2}$$

u_B denotes a column vector of boundary DOF, u_I denotes a column vector of interior DOF, I and 0 are identity and zero matrices, Φ_{IC} are physical displacements of interior DOF in the constrain modes, Φ_{IN} are physical displacements of interior DOF in normal modes, q_C is a column vector of the modal co-ordinates of the constrain modes and q_N a column vector of the modal co-ordinates of the fixed-boundary normal modes [1].

The generalized stiffness and mass matrices corresponding to the Craig-Bampton modal basis are obtained via a modal transformation. The stiffness transformation is

$$K_{GEN} = \Phi^T K \Phi = \begin{pmatrix} I & 0 \\ \Phi_{IC} & \Phi_{IN} \end{pmatrix}^T \begin{pmatrix} K_{BB} & K_{BI} \\ K_{IB} & K_{II} \end{pmatrix} \begin{pmatrix} I & 0 \\ \Phi_{IC} & \Phi_{IN} \end{pmatrix} = \begin{pmatrix} K_{CC} & 0 \\ 0 & K_{NN} \end{pmatrix} \tag{3}$$

and mass transformation is

$$M_{GEN} = \Phi^T M \Phi = \begin{pmatrix} \mathrm{I} & 0 \\ \Phi_{IC} & \Phi_{IN} \end{pmatrix}^T \begin{pmatrix} M_{BB} & M_{BI} \\ M_{IB} & M_{II} \end{pmatrix} \begin{pmatrix} \mathrm{I} & 0 \\ \Phi_{IC} & \Phi_{IN} \end{pmatrix} = \begin{pmatrix} M_{CC} & M_{CN} \\ M_{NC} & M_{NN} \end{pmatrix}, \qquad (4)$$

where the subscripts *I, B, N* and *C* denote interior DOF, boundary DOF, normal mode and constrain mode.

Equations (3) and (4) have a few properties. The submatrices M_{NN} and K_{NN} are diagonal because they are associated with eigenvectors, the matrix K_{GEN} is block diagonal. There is no stiffness coupling between constrain modes and fixed-boundary normal modes. The matrix M_{GEN} is not block diagonal because there is an inertia coupling between the constrain modes and fixed-boundary normal modes [1].

The Craig-Bampton method is a powerful method for tailoring the modal basis to capture both the desired attachment effects and the desired level of dynamic content. However, the raw Craig-Bampton modal basis has certain deficiencies that make it unsuitable for use in a dynamic system simulation. These are:

- Embedded in the Craig-Bampton constrain modes are 6 rigid body DOFs which must be eliminated before the ADAMS analysis because ADAMS provides its own large-motion rigid body DOF.
- The Craig-Bampton constrain modes are the result of a static condensation. These modes do not advertise the dynamic frequency content that they must contribute to the flexible body.
- The Craig-Bampton constrain modes cannot be disabled because it would not be possible to apply constrains to the system.

The problems mentioned above can be easily resolved by applying a simple mathematical operation to the Craig-Bampton modes. The Craig-Bampton constrain modes are not an orthogonal set of modes, as evidenced by the fact that their generalized mass and stiffness matrices M_{GEN} and K_{GEN}, encountered in equations (3) and (4), are not diagonal. By solving an eigenvalue problem

$$K_{GEN}q = \lambda M_{GEN}q, \qquad (5)$$

eigenvectors can be obtained that these can be arranged in a transformation matrix *N* which transforms the Craig-Bampton modal basis to an equivalent, orthogonal basis with modal coordinates q^*

$$\mathrm{N}q^* = q_{\cdot} \qquad (6)$$

The effect on the superposition formula (1) is

$$u = \sum_{i=1}^{M} \Phi_i q_i = \sum_{i=1}^{M} \Phi_i \mathrm{N}q^* = \sum_{i=1}^{M} \Phi_i^* q_i^*, \qquad (7)$$

where Φ_i^* denotes orthogonalized Craig-Bampton modes.

The orthogonalized Craig-Bampton modes are not eigenvectors of the original system. They are eigenvectors of the Craig-Bampton representation of the system and as such they have natural frequencies associated with them. The flexible body reductions are calculated in ANSYS using a user written macro [1].

The virtual engine used for the dynamic solution of a target engine incorporates flexible bodies of crankshafts and a propeller shaft. Figure 3 presents FE model of a crankshaft.
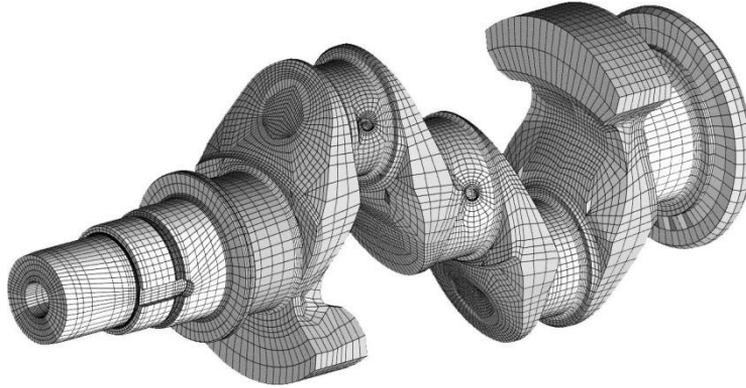
Fig. 3 FE model of the crankshaft

3.2. Rigid Bodies

The other bodies like pistons, piston pins or an engine block are considered as rigid. Compressor including a compressor drive is also incorporated into the model. The compressor is considered as a rigid rotor with reduced inertia moment and a loading moment. Propeller is considered as rigid disc with corresponding inertial moment for initial solutions. Speed reducer consisting of a gear system is also included in the model. Gears are modelled as flexible bodies in one degree of freedom with defined torsion stiffness and damping corresponding to the individual gearing. Radial and tangential forces are also included in the gear model [1].

3.3. Theory Background of Slide Bearing Models

Present computational models enable to describe slide-bearing behaviour in high details. These models are often very complicated and require long solution times even on condition that only one slide bearing model is being solved. The target engine includes a lot of slide bearings, therefore, all model features of slide bearings have to be carefully considered.

The loading capacity of a slide bearing model included in the virtual engine is considered in a radial direction and also incorporates pin tilting, which means that radial forces and moments are included into the solution. For the solution of powertrain part dynamics elastic deformations can be neglected because integral values of pressure (forces and moments) for HD (hydrodynamic) and EHD (elastohydrodynamics) solution are approximately the same. This presumption is very important and it enables a simplification of the solution. On the other hand, the solution cannot be used for a detailed description of the slide bearing. Solutions of tens of EHD slide bearing models simultaneously seem to be extremely difficult and do not provide any fundamental benefits for general dynamics. The virtual engine therefore incorporates a compromise solution using the HD solution with elastic bearing shells and can be named (E)HD approach [1].

An HD approach presumes that shapes of pin and bearing shell are ideal cylindrical parts. The pin and the bearing shell are rigid bodies without any deformations. An oil gap between the pin and the shell is filled up by the oil and gap proportions are small in comparison with pin or bearing shell proportions. Only hydrodynamic frictions occur, lubricating oil is incompressible and oil flow is laminar.

Generally, oil temperature has a significant influence on slide bearing behaviour. Oil temperature is treated as a constant for whole oil film of the bearing. This presumption enables to include temperature influences after the hydrodynamic solution according to temperatures determined from similar engines [1].

In general, if the equation of the motion and Continuity equation [2] are transformed for cylindrical forms of bearing oil gap together with restrictive conditions [2], the behaviour of oil pressure can be described by Reynolds differential equation (7). This frequently used equation is derived for a bearing oil gap and can be written in the form

$$\frac{\partial}{\partial x}\left(\frac{\rho h^3}{12\eta}\frac{\partial p}{\partial x}\right) + \frac{\partial}{\partial y}\left(\frac{\rho h^3}{12\eta}\frac{\partial p}{\partial y}\right) - U\frac{\partial(\rho h)}{\partial x} - \frac{\partial(\rho h)}{\partial t} = 0 \ , \tag{7}$$

where p is pressure, h is oil film gap thickness, η is dynamic viscosity of oil, ρ is oil density and U is an effective velocity.

If the dimensionless oil film gap is used for the Reynolds equations for tangential and radial movements of the pin together with the transformation of pressure [1], then the equation (7) can be rewritten into two separate equations and the final forms of Reynolds equations are

$$\frac{\partial^2 \overline{\Pi}_D}{\partial \varphi^2} + \left(\frac{D}{B}\right)^2 \frac{\partial^2 \overline{\Pi}_D}{\partial Z^2} + a(\varphi,\varepsilon,Z,\gamma,\delta)\overline{\Pi}_D = b_D(\varphi,\varepsilon,Z,\gamma,\delta) \ , \tag{8}$$

$$\frac{\partial^2 \overline{\Pi}_V}{\partial \varphi^2} + \left(\frac{D}{B}\right)^2 \frac{\partial^2 \overline{\Pi}_V}{\partial Z^2} + a(\varphi,\varepsilon,Z,\gamma,\delta)\overline{\Pi}_V = b_V(\varphi,\varepsilon,Z,\gamma,\delta) \ , \tag{9}$$

where R is a shell radius, r is a pin radius, e is a pin eccentricity, γ and δ are pin tilting angles and φ is an angle about pin axis. The following relations can be defined

$$\varphi = \frac{x}{R} = \frac{2x}{D} \ , \quad Z = \frac{2z}{B} \ , \quad \psi = \frac{s}{D} = \frac{R-r}{R} \cong \frac{R-r}{r} \ , \quad \varepsilon = \frac{e}{R-r} , \tag{10}$$

where φ is angle, D is a shell diameter, B is a width of the bearing, Z is dimensionless co-ordinate in bearing axis direction, s is a bearing clearance, ψ is an independent bearing clearance and ε is dimensionless eccentricity. Definitions of the equation terms $a(\varphi,\varepsilon,Z,\gamma,\delta)$, $b_D(\varphi,\varepsilon,Z,\gamma,\delta)$ and $b_V(\varphi,\varepsilon,Z,\gamma,\delta)$ can be found in [1] or [7].
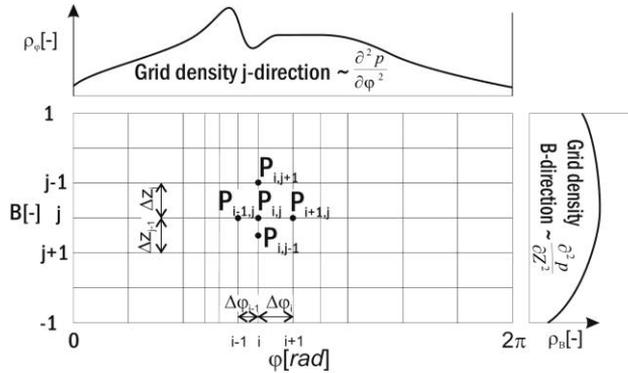

Fig. 4 Computational grid for FDM with variable integration step

Equations (8) and (9) are solved numerically. The FDM (Finite Difference Method) is used for numeric solution. The FDM in basic form uses a constant integration step, however, this strategy can be disadvantageous because in case the pin eccentricities are very high, the oil film pressure becomes concentrated in small areas and it is necessary to use a very small integration step. This leads to higher computational models. Therefore, FDM using variable integration step combining with multigrid strategies is developed. The grid density is changed in dependency on prescribed conditions. Three- point integration scheme has been chosen for the solution because for small integration steps it is very fast and the accuracy is similar to five-point integration scheme. Figure 4 presents an example of computational grid for FDM with a variable integration step [1].

Resulted formula for iterative solution of dimensionless pressure at point i,j is defined as

$$\overline{\Pi}_{i,j_{D,V}} = \frac{\dfrac{\dfrac{1}{\Delta\varphi_i}\overline{\Pi}_{i+1,j} + \dfrac{1}{\Delta\varphi_{i-1}}\overline{\Pi}_{i-1,j}}{\Delta\varphi_j + \Delta\varphi_{j-1}} + 2\dfrac{D^2}{B^2}\dfrac{\dfrac{1}{\Delta Z_j}\overline{\Pi}_{i,j+1} + \dfrac{1}{\Delta Z_{j-1}}\overline{\Pi}_{i,j-1}}{\Delta Z_j + \Delta Z_{j-1}} - b_{D,V}}{\dfrac{2}{\Delta\varphi_j \Delta\varphi_{j-1}} + \dfrac{D^2}{B^2}\dfrac{2}{\Delta Z_j \Delta Z_{j-1}} - a}. \qquad (11)$$

The formula for the numerical solution (11) is different for tangential and radial pin movement only in the term b_D (for tangential pin movement) and b_V (for radial pin movement) respectively.

The solution approach with variable integration steps presumes sufficient density of a solution grid according to pressure differentiations with respect to the bearing angle and bearing width. This strategy enables solving problematic pressure zones in acceptable solution time.

Equation (11) is solved iteratively for the tangential pin movement as well as for the radial pin movement. Initial and boundary conditions are the same for both solutions. The boundary conditions are described in [1] or [7].

The computed pressure distributions have to be transferred to equivalent force systems for a solution in MBS. Pressure on an elementary surface can be imagined as an elementary force dF on this elementary surface dS. Integral values are dimensionless reaction forces F and reaction moments M and can be found by an integration of pressure across the whole bearing surface with coordinates φ a z.

Hydrodynamic databases include integral values for chosen ratios D/B and pin tilting angles. Resulted forces and moments inserted into MBS can be obtained by an inclusion of bearing sizes, bearing clearances, dynamic viscosity and pin kinematic values.

4. Vibration Analysis of Base Cranktrain

The cranktrain dynamics in the range from 1600 rpm to 4000 rpm is solved using the virtual engine and subsequently harmonic analyses of these results are performed. Figure 5 shows harmonic analysis results of crankshaft torsion deformations.

The results show that the intake crankshaft vibrations are much higher, but the power output is lower in comparison with the exhaust crankshaft. The higher vibrations are caused by the presence of a compressor drive located at the intake

crankshaft end. Figure 6 presents harmonic analysis results of propeller shaft torsion deformations.

The results also show the existence of a few resonances in the engine operation speeds, there are the resonances of 2nd, 4th and 6th harmonic orders.

The critical engine speed can be slightly moved depending on propeller and pulley inertia moments, but there is still the necessity to design an appropriate solution enabling a torsion vibration decrease.
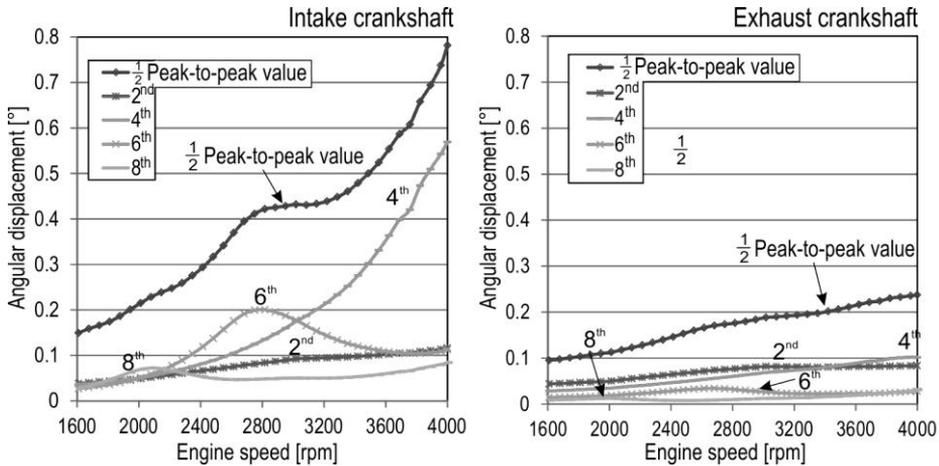

Fig. 5 Harmonic analysis results of crankshaft torsion deformations
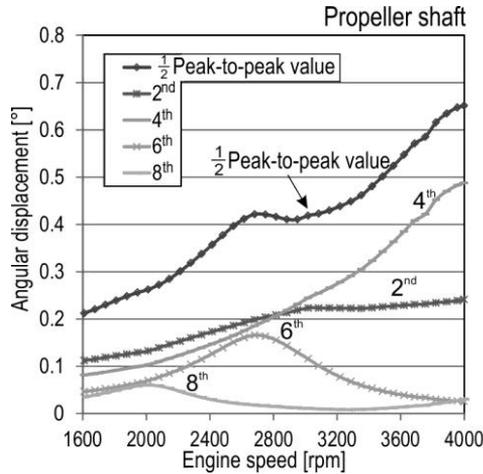
Fig. 6 Harmonic analysis results of propeller shaft

5. Fatigue Analysis of Initial Cranktrain Parts

Powertrain dynamic results are used for a fatigue analysis of main powertrain components. The modal approach of a component stress determination used for fatigue analyses can be applied only to reduced FE bodies. Principles of a component stress determination consist in the combination of dimensionless modal stresses found by a

computational modal analysis and scaled time variable generalized coordinates found by a powertrain dynamic solution. The combination of the dimensionless stresses and the generalized coordinates generates real stresses for each mode. A set of mode stresses gives a total stress for each node of FE body as a function of time. These time variable stresses are used for the component fatigue calculations [4]. Figure 7 demonstrates principles of component stress composition based on FE and MBS results.

Influences like material properties, surface roughness, component sizes, a stress gradient, means stress and so on are additional inputs for fatigue analyses. Fatigue analysis results can be characterized, for example, by safety factors. More information about fatigue analyses can be found in references [5, 6].
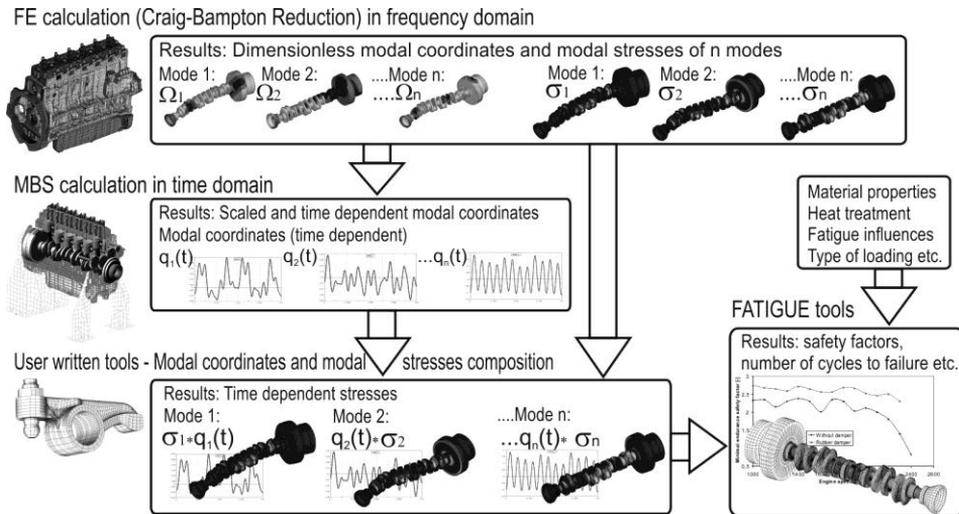
Fig. 7 Principles of component stress composition based on FE and MBS results
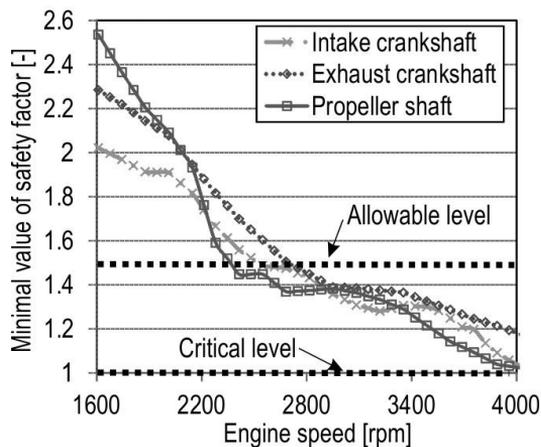

Fig. 8 Minimal values of safety factors for intake and exhaust crankshaft and propeller shaft for whole speed range

The minimal values of crankshaft and propeller shaft safety factors for whole speed range are presented in Figure 8. Low safety factors in higher speed are caused by a combination of high peak values of combustion pressures and high torsion vibrations of the cranktrain. Figure 9 shows fatigue results of intake crankshaft and figure 10 presents fatigue results of propeller shaft, both of the results are for engine speed 3600 rpm.
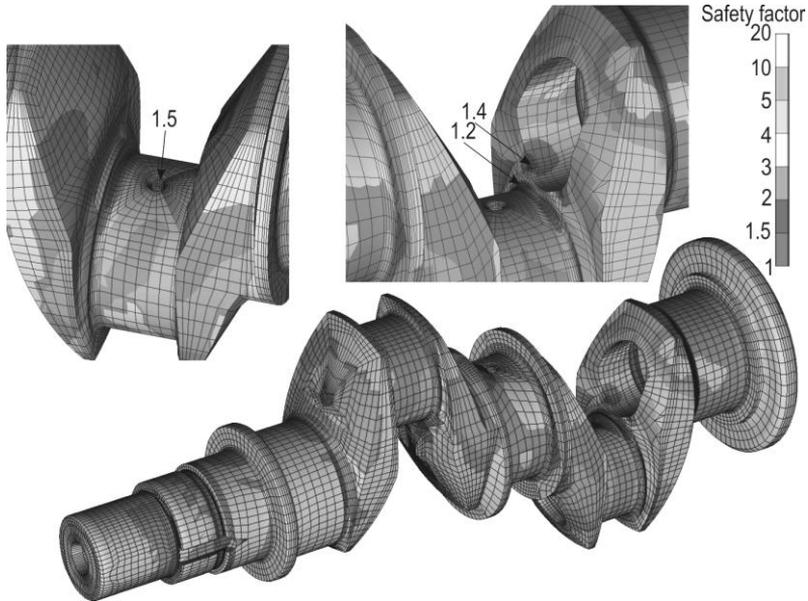
Fig. 9 Safety factor distribution of the intake crankshaft for an engine speed of 3600 rpm
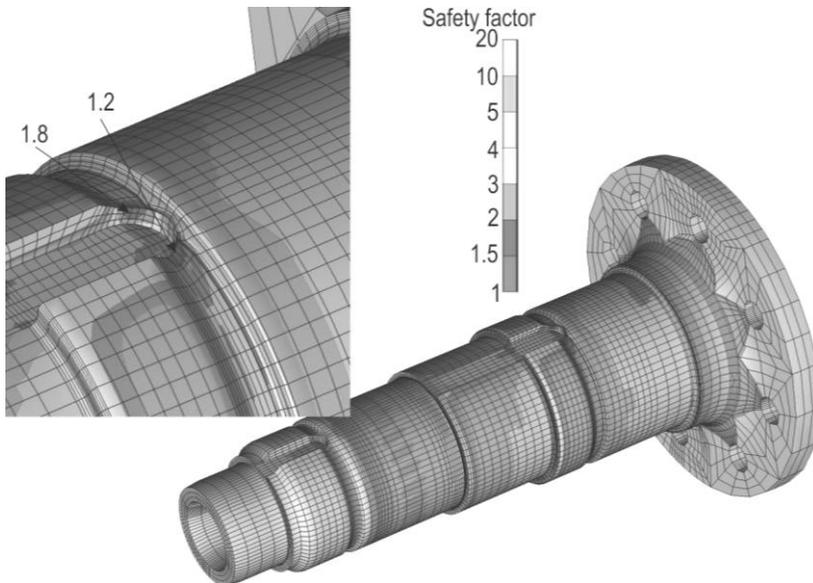
Fig. 10 Safety factor distribution of the propeller shaft for an engine speed of 3600 rpm

The results show that the fatigue of main parts of present design is poor and some design changes have to be implemented.

6. Solution for Vibration Decrease

6.1. New Design of Crankshafts

Crankshaft fatigue problems can be partially solved by a suitable and detailed crankshaft design. For the first stage, five designs different in balance weights and lightweight proposals of the crankshaft were submitted. Because there were higher requirements on crankshaft fatigue, the main emphasis is primarily put on the crankshaft strength and secondarily on crankshaft weight. The requirements reducing bearing loadings are restricted. Figure 11 presents the final design of the crankshaft without any significant lightweight proposals and balance weights. Considering a small-run production of the engine, the crankshaft is supposed to be produced by cutting operations. Casted versions of the crankshaft can be considered in the next phases. [4]
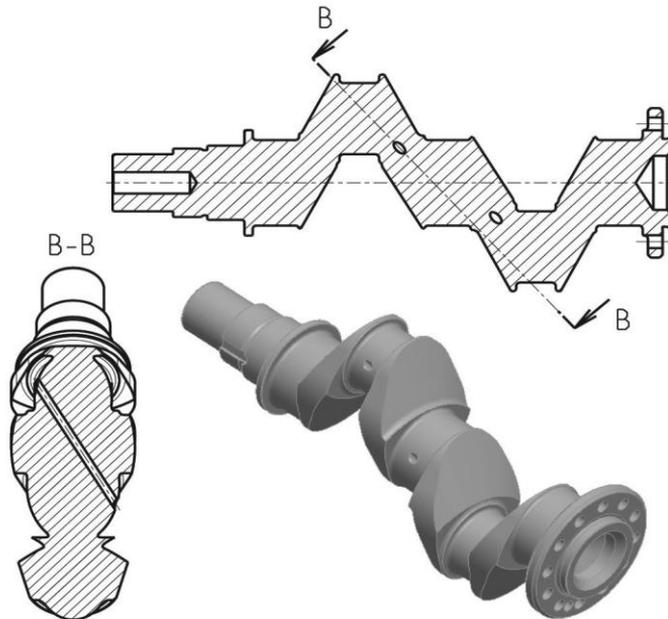

Fig. 11 Final crankshaft design

6.2. Crankshaft Pulley Weight Reduction

The torsion vibrations are influenced by a crankshaft pulley and a compressor. The inertia moment of the compressor cannot be changed, therefore there is only one way to reduce the crankshaft pulley inertia moment and mass. Therefore, magnesium alloys are used for the crankshaft pulley.

Considering the initial design, the shape optimisation is performed using ANSYS optimising tools. Initial and modified designs of the crankshaft pulley are presented in

Figure 12. The resultant inertia moment of the modified crankshaft pulley is reduced by more than 32 % and the pulley mass is reduced by more than 28 % in comparison with the initial design made of aluminium alloys.
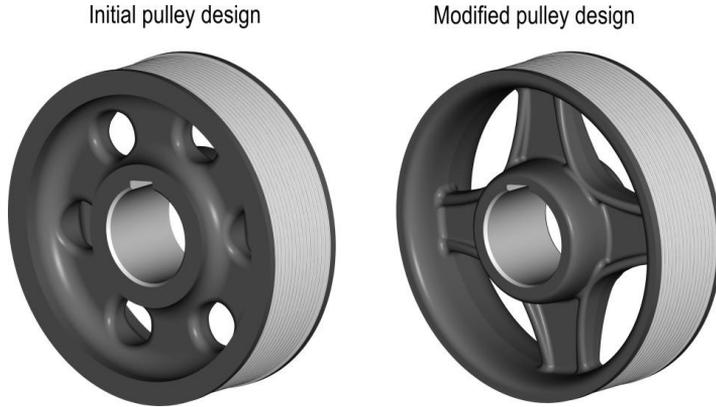

Fig. 12 Initial and modified design of crankshaft pulley

6.3. Torsional Damper Application

Torsion vibration can be also reduced by the application of a torsional damper or a flexible attached crankshaft pulley. The proper solution of the flexible attached pulley re-tunes the torsion system and this change restricts dangerous resonances in the whole engine speed range. The flexible attached pulley design has to be equipped with a radial bearing to restrict radial deformations from compressor drive forces. Figure 13 presents a harmonic analysis result comparison of half of peak-to-peak values of intake crankshaft torsion deformations of the initial and the modified cranktrain design incorporating an isolation pulley. The results show that the torsion vibrations have been highly reduced.
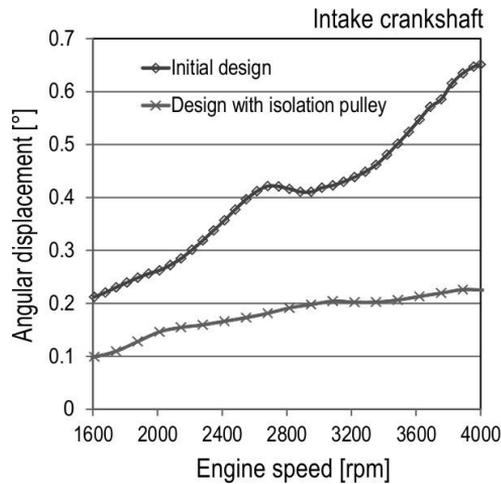

Fig. 13 Harmonic analysis result comparison of half of peak-to-peak values of intake crankshaft torsion deformations of the initial and the modified cranktrain design incorporating isolation pulley

However, the resulted crankshaft fatigue has not improved as much as torsional vibrations have been reduced, because the crankshaft fatigue is also influenced by high values of combustion pressures and these are not changed.

7. Fatigue Analysis of Modified Cranktrain Parts

Figure 14 presents the fatigue results of the intake crankshaft and the propeller shaft considering modified design changes. The minimal values of safety factors are above the allowable values and the new designs are validated.
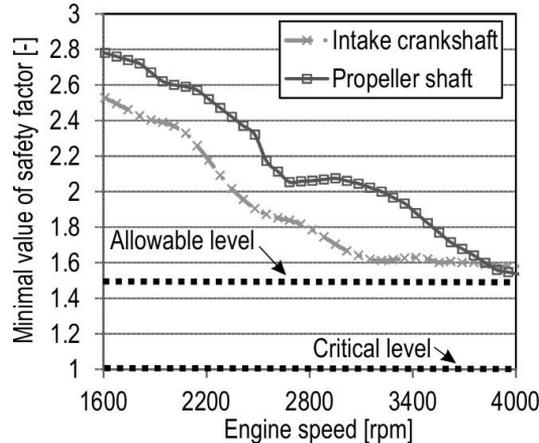

Fig. 14 Minimal values of safety factors for modified intake crankshaft and propeller shaft for whole speed range

8. CONCLUSION

In the stage of the engine development, a high number of computational approaches have been utilized to reduce the cost and accelerate the development. The computational methods presented in this paper represent modern computational methods which can be used in the initial phase of a cranktrain development and also in the phase of parameter tuning of an existing cranktrain. These methods often require at least some initial design of the main engine parts, mainly those which are highly loaded. These methods enable to design the engine parts in high details satisfying the target criteria without long and expensive measurements.

The resultant target diesel engine will incorporate unconventional cranktrain arrangement supplemented by modern features, such as a turbocharger in combination with supercharger and other modern parts. All these features will enable high power output with low specific engine weight and low fuel consumption. The engine potentials enable to use the engine in the area of military/commercial aircraft or helicopters, and with some modifications in the area of military generator sets.

References

[1]   NOVOTNÝ, P. and PÍŠTĚK, V. New Efficient Methods for Powertrain Vibration Analysis. *Proceedings of the Institution of Mechanical Engineers – Part D:*

Journal of Automobile Engineering, 2010, vol. 224, no. 5, p. 611-629. ISSN 0954-4070.

[2]   BUTENSCHÖN, HJ. *Das hydrodynamische, zylindrische Gleitlager endlicher Breite unter instationärer Belastung* [PhD Thesis]. Karlsruhe (Germany) : Universität Karlsruhe, 1976.

[3]   REBBERT, M. *Simulation der Kurbewellendynamik unter Berücksichtigung der hydrodynamischen Lagerung zur Lösung motorakusticher Fragen* [PhD Thesis]. Aachen (Germany) : Rheinisch-Westfälische Technische Hochschule, 2003.

[4]   NOVOTNÝ, P., PÍŠTĚK, V., DRÁPAL, L. and AMBRÓZ, R. Cranktrain Development of Aircraft Diesel Engine. In *XLI. International Scientific Conference of Czech and Slovak University Departments and Institutions Dealing with the Research of Combustion Engines*. Liberec : Technická universita v Liberci, 2010. p. 212-222. ISBN 978-80-7372-632-4.

[5]   HOLLMANN, C. *Die Übertragbarkeit von Schwingfestigkeits-Eigenschaften im Örtlichen Konzept* [PhD Thesis]. Dresden (Germany) : Technische Universität Dresden, 1971.

[6]   GAIER, C. and DANNBAUER. H. Fatigue Analysis of Multiaxially Loaded Components with the FE-Postprocessor FEMFAT-MAX. *ESIS Publication*, 2003, vol. 31, p. 223-240.

[7]   NOVOTNÝ, P. *Virtual Engine – A Tool for Powertrain Development* [Inaugural Dissertation]. Brno : Brno University of Technology, 2009.

Acknowledgement